TECHNICAL JUSTIFICATION FOR ELIMINATING THF
MID-CYCLE INSPECTION OF THE FEEDWATER NOZZLE (N4A)
TO SAFE END WELD INDICATION AT THE RIVER BEND PLANT
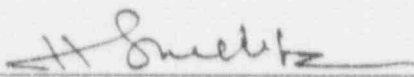
July 1991

Prepared for

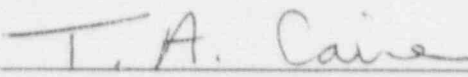Gulf States Utilities Company
St. Francisville, Louisiana

Prepared by

GE Nuclear Energy
175 Curtner Ave.
San Jose, CA 95125

TECHNICAL JUSTIFICATION FOR ELIMINATING THE
MID-CYCLE INSPECTION OF THE FEEDWATER NOZZLE (N4A)
TO SAFE END WELD INDICATION AT THE RIVER BEND PLANT

July 1991

Prepared by: _____

H.S. Mehta, Principal Engineer
Materials Monitoring and Structural
Analysis Services

Reviewed by: _____

T.A. Caine, Senior Engineer
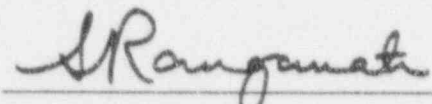Materials Monitoring and Structural
Analysis Services

Approved by: _____

S. Ranganath, Manager
Materials Monitoring and Structural
Analysis Services

TABLE OF CONTENTS

TABLE OF CONTENTS (CONT'D)

1.0 BACKGROUND

As part of the ultrasonic inspection of Alloy-182 weldments in River. end station, an indication approximately 6-inches long and peak depth of 0.20 inches was discovered in March 1989 in the Alloy-182 weld butter of the feedwater nozzle (N4A) to safe end weld. Figure 1-1 shows the nozzle weld configuration and the location of the indication. A crack growth evaluation was performed assuming that the observed indication was due to an active IGSCC crack. The predicted crack size at the end of the next fuel cycle was determined assuming two crack growth rates (an upper bound value and an expected realistic value) and compared with the ASME Code allowable flaw size [1-1]. The analysis confirmed that continued plant operation could be justified and that the required code margins were maintained. In addition to the analysis, a mid-cycle examination of the indication was also planned to provide confirmatory evidence of the conservatism of the crack growth rate assumptions. Based on the results of the analysis and the plans for a mid-cycle ultrasonic inspection, the NRC allowed plant startup without repair.

In March 1990 ultrasonic (mid-cycle) examinations were performed on the weld in order to detect any changes in the dimensions of a planar type reflector detected during the second refueling outage (RF-2). The results of these examination showed some increase in length but no detectable change in depth from initial detection and sizing to the mid-cycle outage. At the end of the third fuel cycle (November, 1990), the weld was again examined to determine changes in the crack size. Ultrasonic examinations were performed using both manual and automatic techniques. The examinations performed during the third refueling outage (RF-3) showed changes in depth, as well as length, compared to those seen during the previous examination. A breakdown of the manual and automated results for the initial, midcycle and the latest inspections are shown in Table 1-1.

Based on the results of the RF-3 examinations, the reflector is 7.7" long, exhibiting an increase in length of 1.6" from March 1989 to November 1990.

The depth has increased from 0.20" (18% TWD) to 0.33" (30% TWD) in the deepest areas. These results were confirmed using several different transducers along with the P-Scan Automated System to obtain accurate, finite through-wall dimensions. The final depth recorded by the P-Scan was 30% at the deepest location with an average depth of 15% to 20% over the remainder of the reflector. Figure 1-2 shows a depth profile of the indication in March 1989 and in November 1990.

A fracture mechanics analysis [1-2] was performed to determine acceptability for the next fuel cycle (i.e., through March 1992). It was concluded that even for the bounding crack growth assumptions, continued operation could be justified for the duration of the current fuel cycle lasting until March 1992. Nevertheless, to provide additional conservatism Gulf States Utilities (GSU) agreed to perform a mid-cycle inspection in September 1991.

Since then, GSU has taken and will take several actions which will significantly reduce the need for, as well as the value of, a mid-cycle inspection. These actions include:

o   Plans to implement more restrictive technical specification limits on unidentified leak rate. This will provide added assurance of leak margin so that even under the most unlikely circumstance of the crack growth being excessive, a potential leak could be detected readily.

o   Added emphasis on maintaining the water chemistry to assure that the BWR Industry/EPRI guidelines are not only met but improved upon. GSU implemented modifications to improve RWCU system performance during RF-3.

In view of these corrective actions and the radiation exposure, as well as, the added plant downtime resulting from the inspection, it is concluded that the mid-cycle inspection is unnecessary. This is especially true when one considers the fact that the indication has been shown to be acceptable for continued operation through March 1992.

1-2

This report provides the technical justification for the elimination of the mid-cycle examination requirement. It confirms that even with conservative assumptions on crack growth rates based on the UT, acceptable code margins are maintained for the current cycle. Even if the crack growth rate is higher than expected, a potential through-wall crack can be tolerated and leak-before-break is maintained. The current analysis also assumes that conservative flux weld criteria apply, even through available data suggests that Alloy-182 does not have the toughness concerns associated with submerged arc stainless steel weldments.

1.1 References

1-1 "Evaluation of the Indication in the River Bend Feedwater Nozzle to Safe End Weld," SASR # 89-37, DRF # 137-0010, GE Nuclear Energy, May 1989.

2-1 "Reassessment of the Indication in the River Bend Feedwater Nozzle (N4A) to Safe End Weld," SASR # 90-98, DRF # 137-0010, GE Nuclear Energy, November 1990.

Table 1-1 UT Inspection Comparison

	APRIL 1989	MARCH 1990	NOVEMBER 1990
LENGTH	6.125" MANUAL (EBASCO)	6.625" MANUAL	7.7" MANUAL
	GEOMETRIC (GE SMART)	6.625" P-SCAN	7.7" P-SCAN
DEPTH	20% MANUAL PLANAR (EBASCO)	20% / 18% MANUAL	30% MANUAL
	GEOMETRIC (GE SMART)	20% P-SCAN	30% P-SCAN

NOZZLE N4A
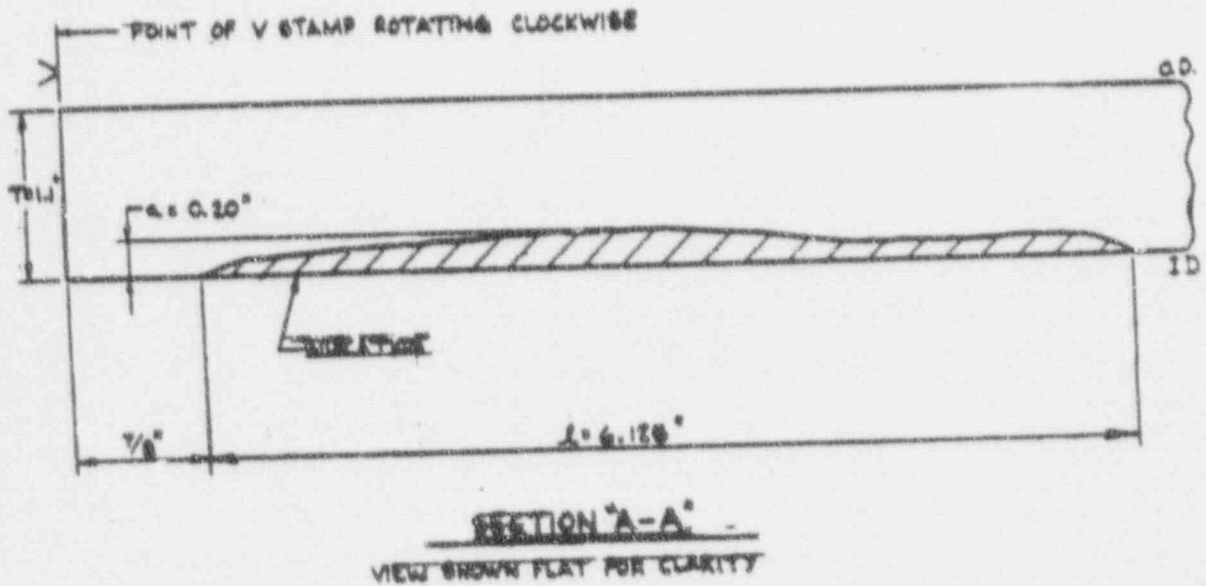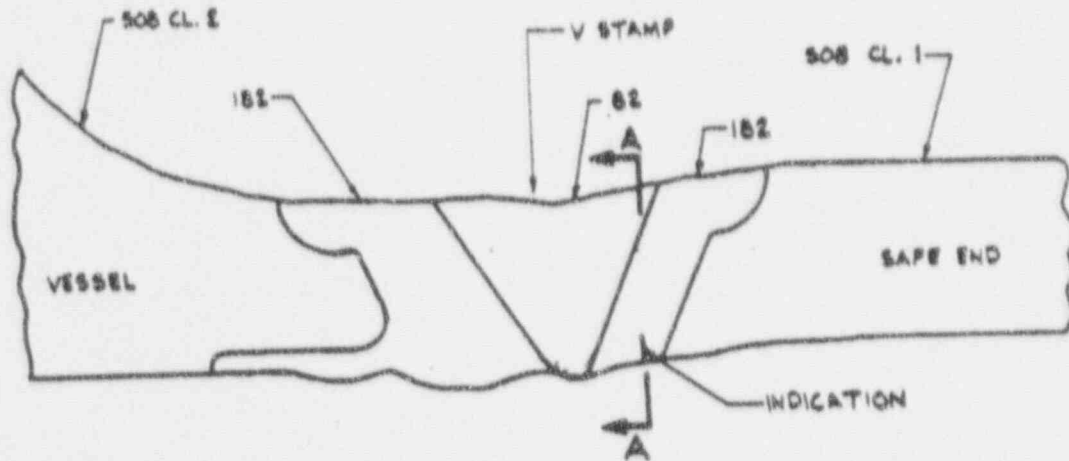

Figure 1-1 N4A weld Geometry and 1989 UT Indication Sizing
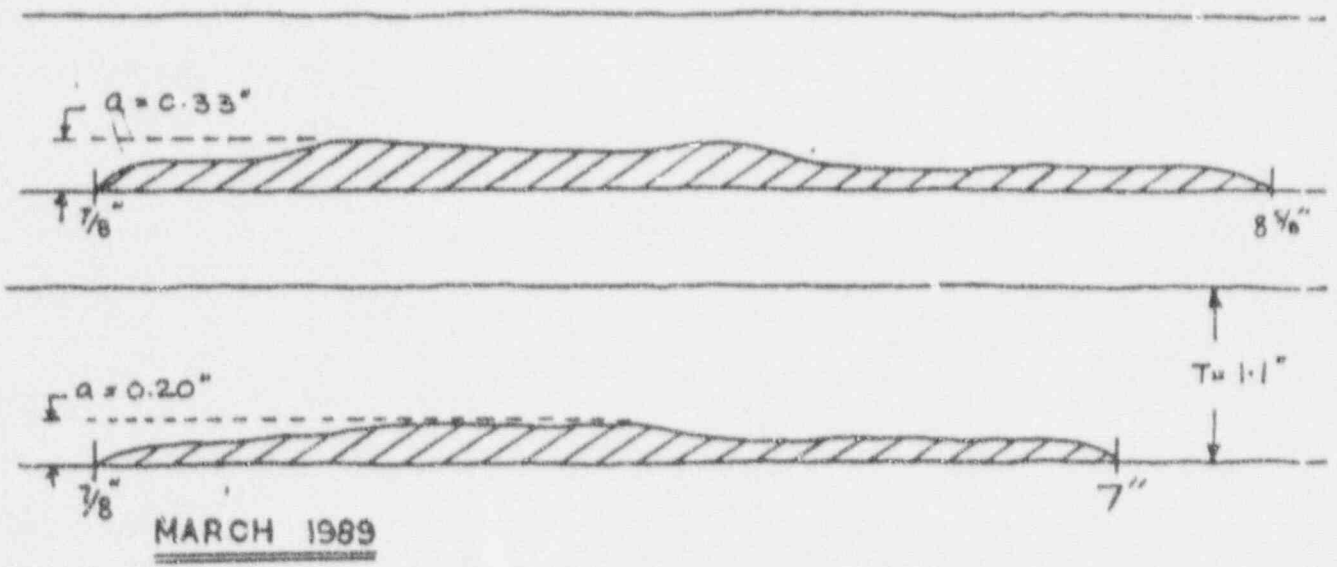
Figure 1-2 Comparison of UT Sizing in March 1989 and November 1990.

2.0 CHEMISTRY CONDITIONS IN THE THERMAL SLEEVE ANNULUS

Since IGSCC growth rates are dependent on the flow conditions, it is useful to know whether crevice conditions exist in the annulus region. Clearly, if it can be shown that there is sufficient flow in the annulus and that the water environment is refreshed periodically, one can conclude that crevice conditions do not exist.

2.1 GE Annulus Region Studies

There have been two major studies on modeling the hydraulic conditions in the thermal sleeve annulus region. The first study conducted by GE [2-1 and 2-2] involved the recirculation nozzle thermal sleeve using both scale model tests (Fig. 2-1) and analytical solutions. The tests used quarter scale modeling of the downcomer and the thermal sleeve annulus and used dye injection and high speed photography. Two annulus gaps were studied - equivalent to 0.13 in. and 0.4 in. in a BWR. The effect of alignment pads was also included. The results (Fig. 2-2 and 2-3) showed that even for the worst gap (0.032 inch in the model or 0.13 inch in the BWR), the annulus flushed in 5 minutes in the test scaling to 20 minutes in the reactor. The GE study also included analytical solution of fluid flow equations to determine oxygen depletion kinetics. The analysis results where shown to be in agreement with the experimental results. The solutions showed no oxygen depletion in any of the cases studied (including annulus gaps of 0.19 inch and lengths up to 19 in.). The absence of oxygen depletion essentially confirms that crevice conditions did not exist in the annulus.

2.2 MIT Annulus Flow Study

More recently scaled model tests were run at Massachusetts Institute of Technology (MIT) in a test program sponsored by EPRI [2-3]. The test simulated a 1/9 scale nozzle-thermal sleeve annulus and investigated two equivalent annulus gaps - 0.2 inch and 0.5 inch. Table 2-1 shows the results of the test for the 0.5 in annulus case. It is seen that the annulus region was flushed

out in less than 2 hours. Figure 2-3 shows calculated PH as a function of exchange rate. It is seen that as long as the annulus is flushed once in 24 hours (turnover of once a day) the water chemistry does not represent creviced condition. The test results show flushing rates well in excess of this threshold value confirming that the annulus is not a crevice.

The test programs addressed the recirc inlet nozzle areas where the annulus gaps vary flow 0.2 in. to 0.5 in. For the River Bend feedwater nozzle thermal sleeve (Fig. 2-4) the annulus gap is 0.625 inch, which exceeds the gap sizes in the recirculation nozzle. Clearly the results of the test programs are conservative when applied to the River Bend FW nozzle and confirm the absence of crevice conditions.

2.3 Effect of Crud on Chemistry/Crack Growth

The next issue to be considered is the potential effect of crud on the chemistry/crack growth conditions. In general, the crud must be adherent to generate crevice conditions. Low pressure flushes in BWR's have shown that the crud, if any, is loose and comes off readily in the form of a turbid cloud. Similar crud behavior was observed in the inreactor crack growth rate studies conducted by GE at the Dresden Unit 2 reactor.

Although there was a significant amount of crud in the vicinity of the specimens, the measured crack growth rates in the in-reactor tests were not different from the values observed in similar laboratory tests where crud conditions did not exist. This provides indirect confirmation on the benign role of crud as far as crevice condition or crack growth rates are concerned.

2.4 Conductivity and ECP Conditions

Given that creviced conditions do not exist, the next question concerns what the chemistry is in the annulus. Studies using the GE-Harwell model show that the effective ECP in the region of the Feedwater Nozzle annulus may range from 100-200 mV.SHE. For the purpose of this analysis a value of 150 mV.SHE will be used. Figure 2-5 shows conductivity data as a function of time. The average

conductivity for the current fuel cycle is 0.17 μs/cm which is below the administrative limit of 0.2 μS/cm. Knowing the ECP and the associated conductivity, crack growth rate predictions can be made.

2.5 References

2-1 Choe, H., "Recirculation Inlet Nozzle Annulus Flow Visualization Test," NEDE-21995, General Electric Company, October 1978.

2-2 Choe, H., "Numerical Analysis on Flow Pattern and Oxygen Concentration Distribution in BWR Recirculation Inlet Nozzle Annulus," NEDE-24663, General Electric Company, May 1979.

2-3 Chun, J.H., "Flow Visualization of BWR Inlet Safe End Annulus," Draft Report EPRI RP 2006-16, Electric Power research Institute, March 1991.

Blockage	Flowrate (gpm)	Flow Speed (ft/s)	Reynolds Number	Time to Flush Out (min)	
				Model	BWR
0%	20	2.6	0.52×10^5	6	148
	50	6.5	1.3×10^5	5	123
	77	10	2.0×10^5	5	123
50%	20	2.6	0.52×10^5	3	74
	50	6.5	1.3×10^5	3	74
	77	10	2.0×10^5	2	49
90%	20	2.6	0.52×10^5	4	99
	50	6.5	1.3×10^5	3	74
	77	10	2.0×10^5	3	74
90% with 2.9" length	20	2.6	0.52×10^5	2	49
	50	6.5	1.3×10^5	2	49
	77	10	2.0×10^5	2	49

INLET THERMAL SLEEVE BENT UPWARD

Table 2-1 Approximate Time to Flush Out the Annulus at
0.055 Inch Width and 7 Inches Length
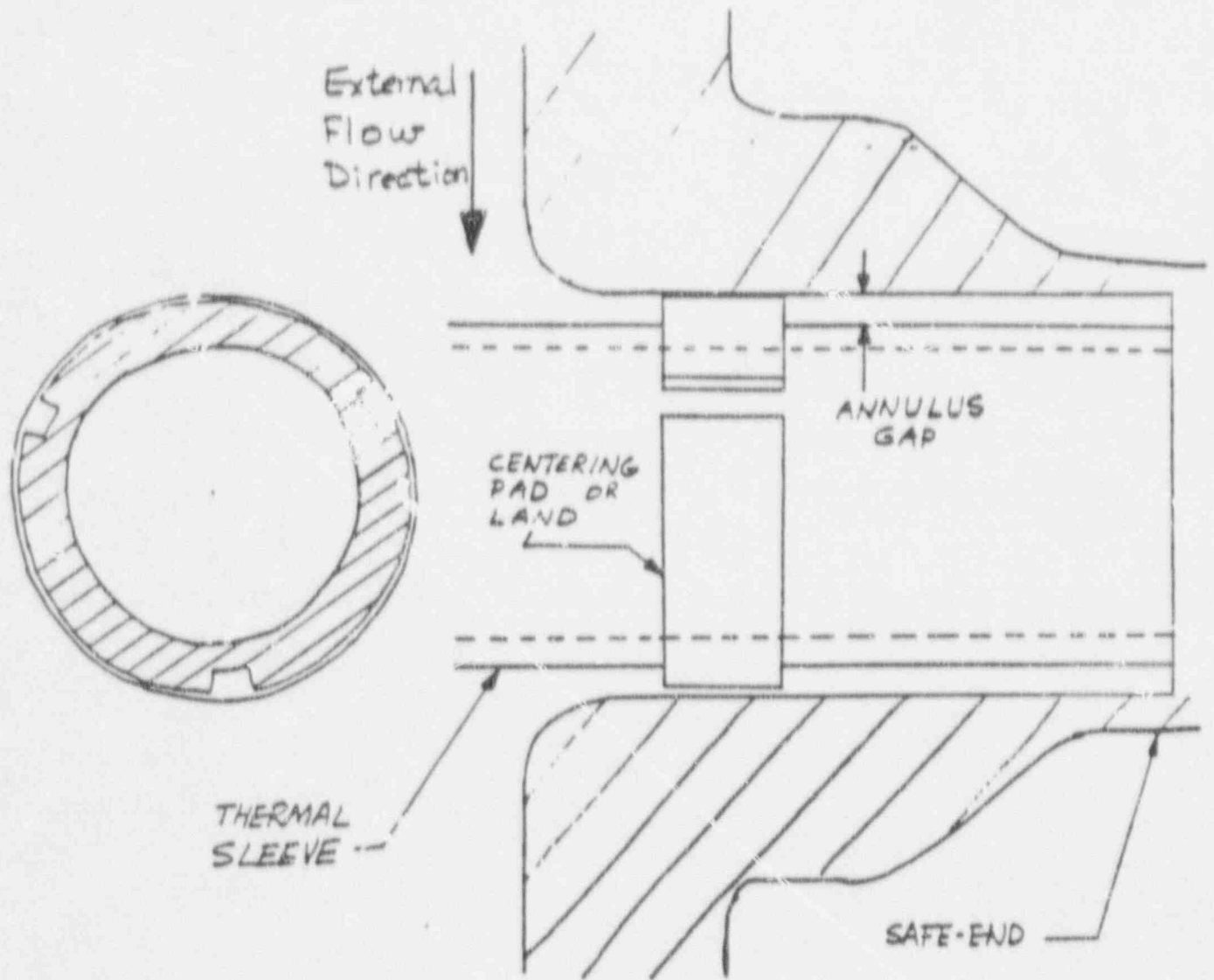
Figure 2-1 Recirculation Inlet Geometry

TEST NUMBER 7

TEST NUMBERS 8 AND 9 ARE SAME AS TEST NUMBER 7

VELOCITY, 0.32 INCH/SEC
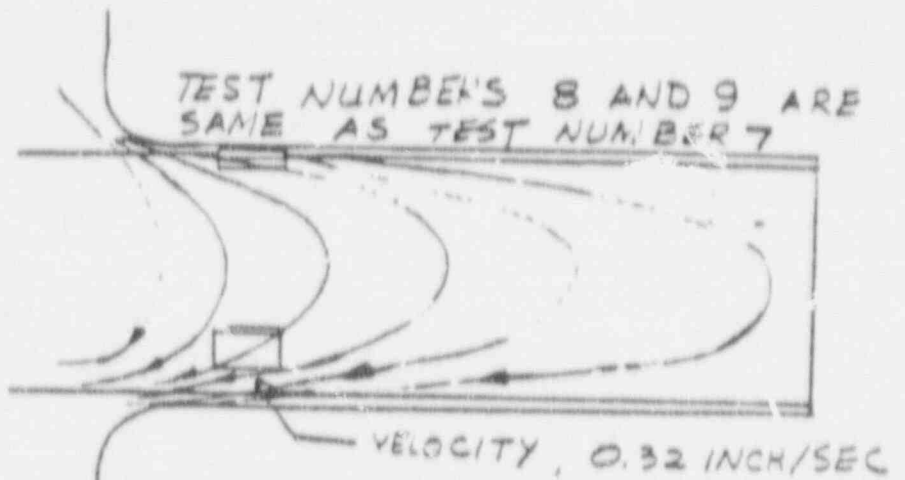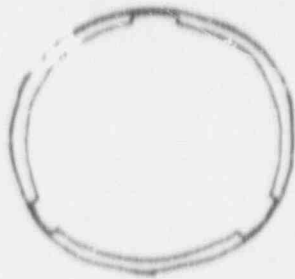
TEST NUMBER 1

TEST NUMBER 3 IS SAME AS TEST NUMBER 1

VELOCITY, 2 INCHES/SEC

TEST NUMBER 2

SAME AS TEST NUMBER 1 EXCEPT THE FOLLOWING MEASURE-MENT

0.4 IN/SEC

0.65 IN
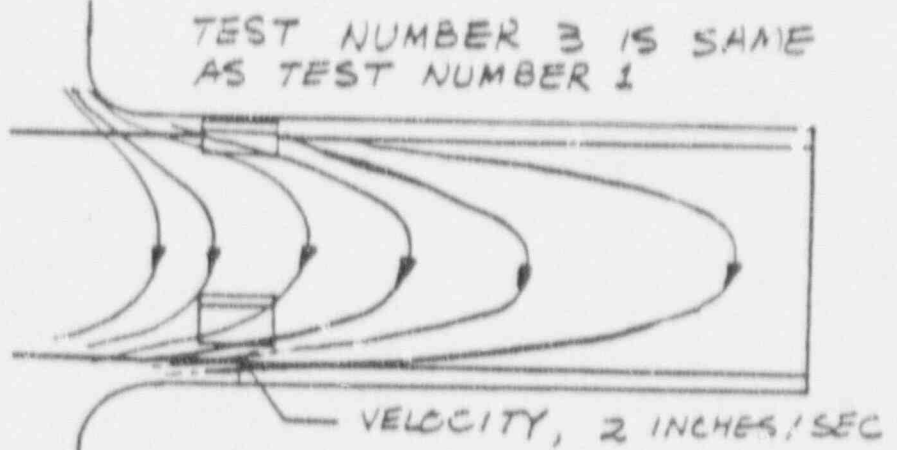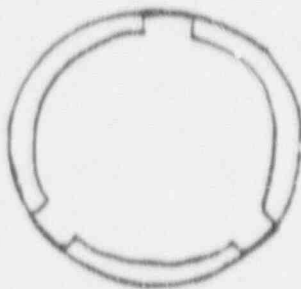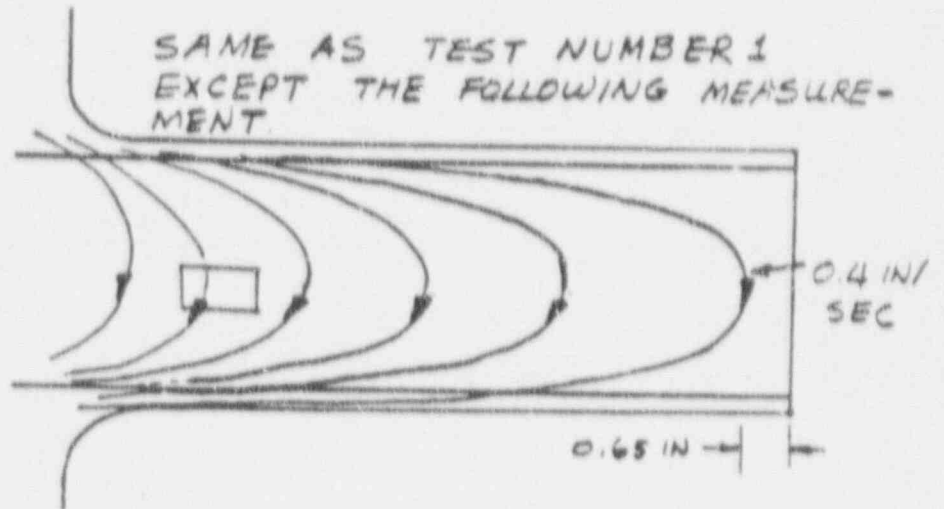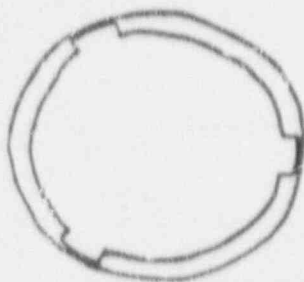
Figure 2-2 Test Results with 60° Land Angle

Effe t of Water Exchange Rate
on Calculated Annulus pH
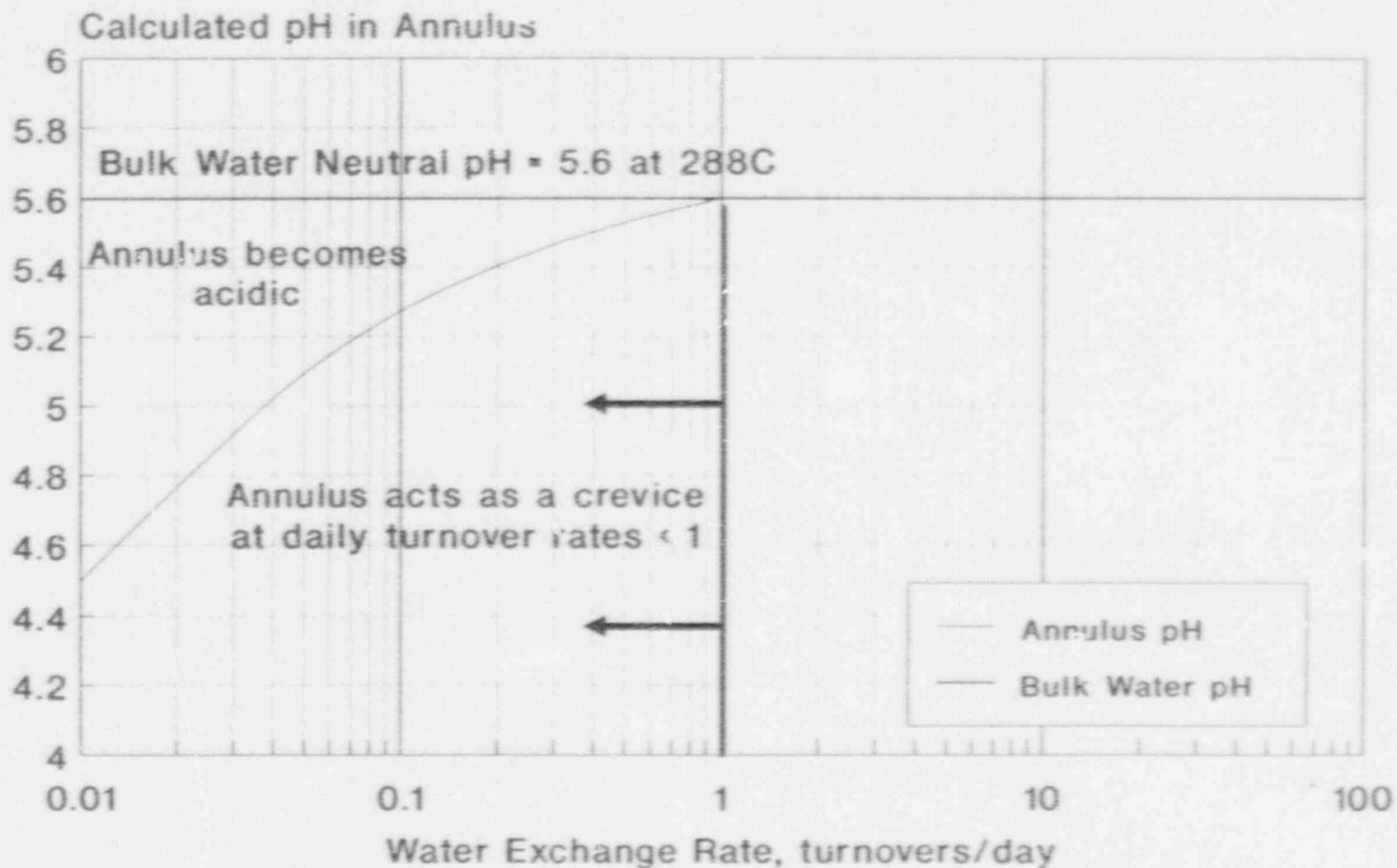
288C, 250 ppb O2

Figure 2-3
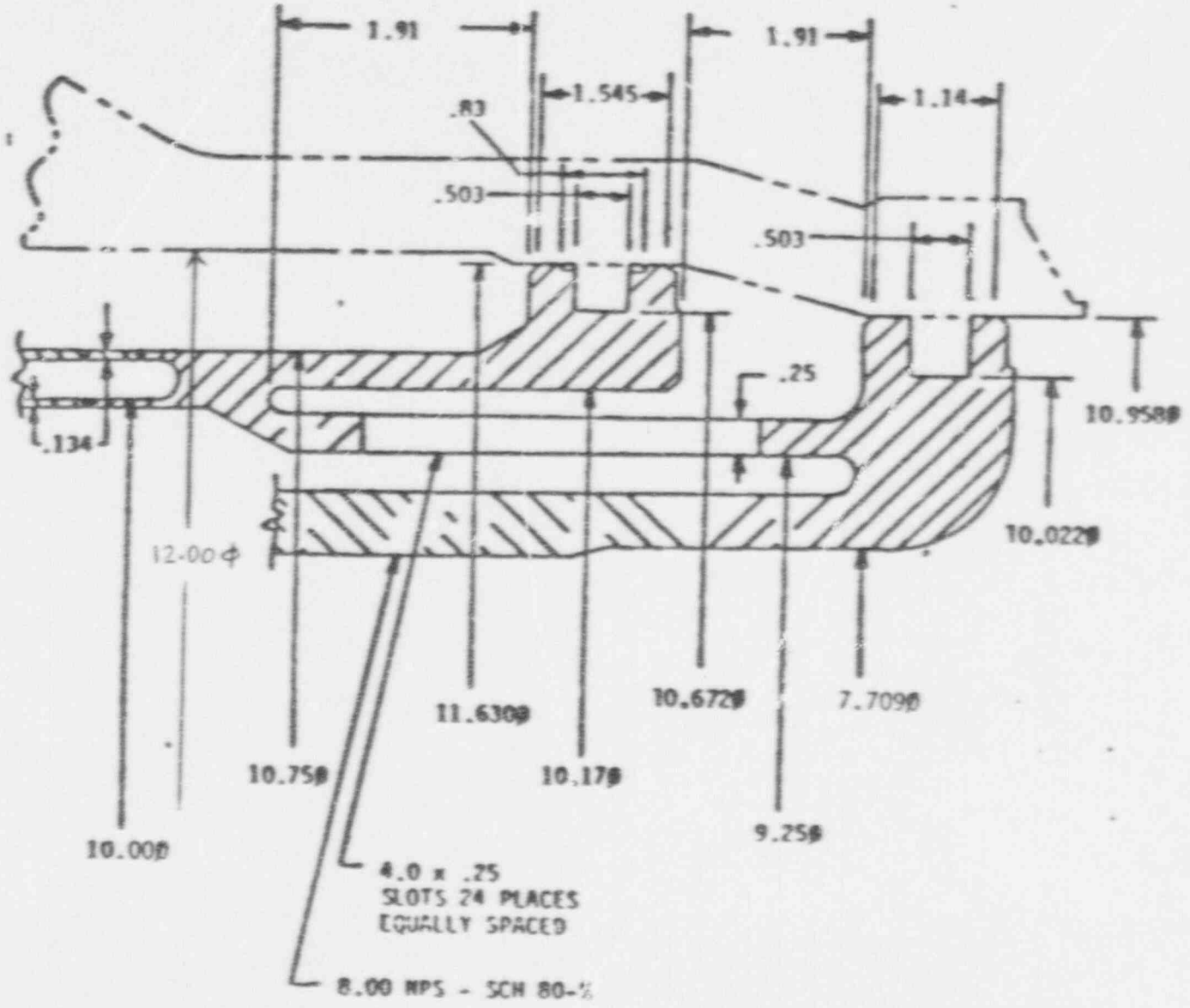
Figure 2-4 Feedwater Nozzle Annulus Geometry

RIVER BEND NUCLEAR STATION – CHEMISTRY DEPARTMENT
REVIEW OF FUEL CYCLE 4 REACTOR WATER CHEMISTRY

DECEMBER 1, 1990 – MAY 21, 1991

River Bend RCS System Conductivity
1991 Goal – 0.14 uS   Fuel Cycle 4 Average – 0.17 uS

ADMIN LIMIT

1991 GOAL

River Bend RCS System Sulfates
Admin Limit – 15 ppb   Fuel Cycle 4 Average – 5.1 ppb

ADMIN LIMIT

FUEL CYCLE 4   (12/01/90 – 05/21/91)
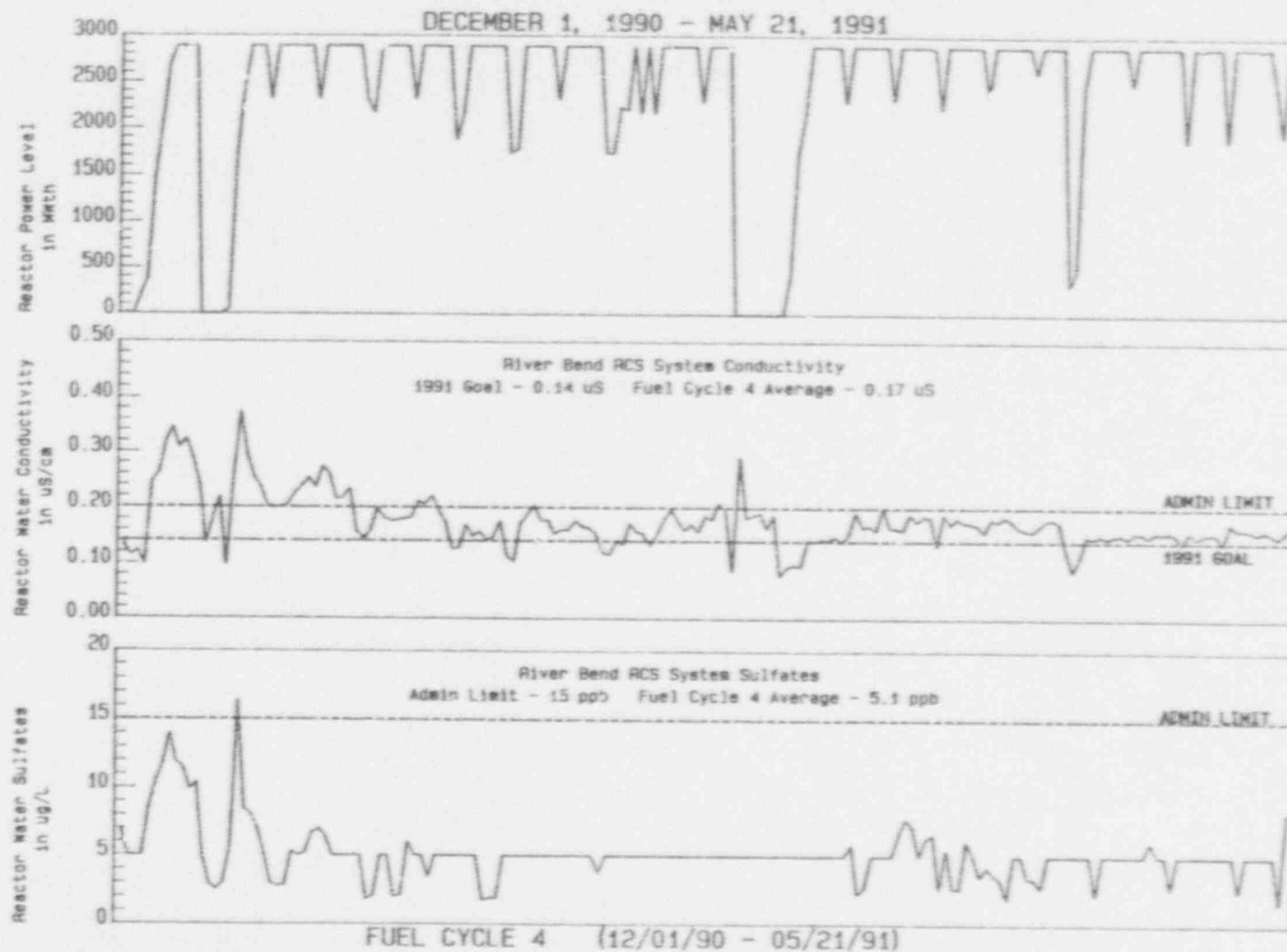
Figure 2-5

3.0 DISCUSSION ON CRACK GROWTH RATES

GE has performed crack growth tests on Alloy-182 in the laboratory with simulated BWR environment and also in several operating BWRs with Crack Arrest/Advance Verification Systems (CAVS). Table 3-1 presents a summary of the GE test results. Several observations can be made from this data:

The laboratory data gave the highest crack growth rates mainly because of the high conductivity, active primary loading and repeated load cycling. All of these factors are known to accelerate crack growth rate. For example, based on GE model described later in section 3.2, the predicted crack growth rate at a conductivity of 0.5 μS/cm (typical for lab tests) can be up to 8 times greater than that at a conductivity of 0.17 μS/cm (average for the River Bend station). Clearly, the higher conductivity in the lab testing is a major accelerant on crack growth rates. Similarly, it is also known th ' dead weight loading (as opposed to displacement/ restraint governed weld residual stresses) and repeated cycling can further increase crack growth rates.

The CAVS growth rates are lower but are still conservative in that the sustained K values are due to dead weight loading instead of displacement governed stresses.

The data show growth rates leveling beyond K values of approximately 25 Ksi√in. This is consistent with classic SCC models for stage III behavior where plateau growth rates are observed. In this region the primary driving force for crack growth is not mechanical in nature but related to other processes occurring at the crack tip such as electrochemical, mass transport diffusion and adsorption.

Figure 3-1 shows the GE crack growth rate data (based mostly on the conservative laboratory tests). As stated earlier, the laboratory tests were done at an average conductivity of 0.5 μS/cm, which represents an extreme water

chemistry condition that would violate BWR industry guidelines. In Figure 3-1, a band was drawn to account for potential data scatter and an upper bound plateau crack growth rate of 5×10^{-5} in/hour was postulated.

Earlier analysis [3-1] used an upper bound value of 5×10^{-5} in/hour based on this data. An 'expected' value of 2×10^{-5} in/hour was also used in Reference 3-1 to represent a nominal crack growth assessment. Since the upper bound value of 5×10^{-5} in/hour (or 0.4 in/year) is unreasonable in relation to field data for BWR conditions, it is appropriate to come up with more realistic crack growth rate values for use in the structural integrity assessments.

Expected crack growth rates in the thermal sleeve annulus can be estimated based on three criteria (i) UT depth estimates (ii) predictions using the GE IGSCC model and (iii) In-plant crack growth rates from monitoring systems in several operating plants.

3.1 UT Based Crack Growth Rates

The UT measured increment in crack depth during fuel cycle 3 was a change from 0.20 to 0.33 inches in approximately 12,000 hours of operation. This translates to growth rate of approximately 1×10^{-5} in/hour. If however, one conservatively uses the change from the mid-cycle inspection to the end of fuel cycle 3, the effective growth rate is 0.13 inches in about 4500 hours or 2.9×10^{-5} in/hour. These two values represent the bounding range that will be used for crack growth analysis.

3.2 Predictions Using the GE IGSCC Model

Andresen [3-2 and 3-3] has shown that the predictive model developed by GE CR&D for stainless steel can be used for Alloy-182 also with an electrochemical potentiokinetic reactivation (EPR) value of 15 Coulombs/cm^2. Figure 3-2 shows the predictions of the model for two selected ECP values (50 and 150 mV) as a function of conductivity. In-reactor data from crack monitoring systems and laboratory data are also shown in the plot. It is seen that the predicted crack growth rate corresponding to the measured River Bend Station average

conductivity of 0.17 μS/cm and ECP of 150 mV,SHE is approximately 3×10^{-5} in/hr. Table 3-1 shows measured crack growth rates reported by Andresen [3-2]. The only case (Andresen Test No. 1 in Table 3-1) where a slightly higher growth rate was measured was a cyclic high R ratio (ratio of the minimum K to maximum K) test with 7000 ppb oxygen. This result is not unreasonable since the test involved more severe cycling and high oxygen concentration.

3.3 Crack Growth Rates Based on CAVS Measurements

GE crack advance verification systems have been used to measure in-plant crack growth rates in Alloy-182 specimens. The 1-inch Compact Tension Specimens were precracked with IGSCC and subjected to dead weight loading. Crack growth rates were measured using the reversing DC potential difference technique. Results of the CAVS measurement show crack growth rates of up to 2.8×10^{-5} in/hour. This is essentially the same as the UT based growth rate of 2.9×10^{-5} in/hour.

Three different methods have been used to estimate the growth rates. It is interesting to note that all three methods suggest a bounding growth rate of approximately 3×10^{-5} in/hour. For the purposes of the analysis, we will use the UT measured range of crack growth rates 1×10^{-5} in/hour and 2.9×10^{-5} in/hour.

3.4 References

3-1 "Evaluation of the Indication in the River Bend Feedwater Nozzle to Safe End Weld," DRF # 137-0010, SASR # 89-37, May 1989.

3-2 Andresen, P.L.,"Observation and Prediction of the Effects of Water Chemistry and Mechanics on Environmentally Assisted Cracking of Inconel 182 Weld Metal and 600," Corrosion-NACE, vol. 44, June 1988.

3-3 Andresen, P.L.,"Fracture Mechanics Data and Modeling of Environmental Cracking of Nickel-Base Alloys in High Temperature Water," Paper No. 44, Presented at the NACE Annual Conference and Corrosion Show, March 1991.

TABLE 3-1

GE LABORATORY AND CAVS DATA ON ALLOY 182 SCC GROWTH RATES AT 550F

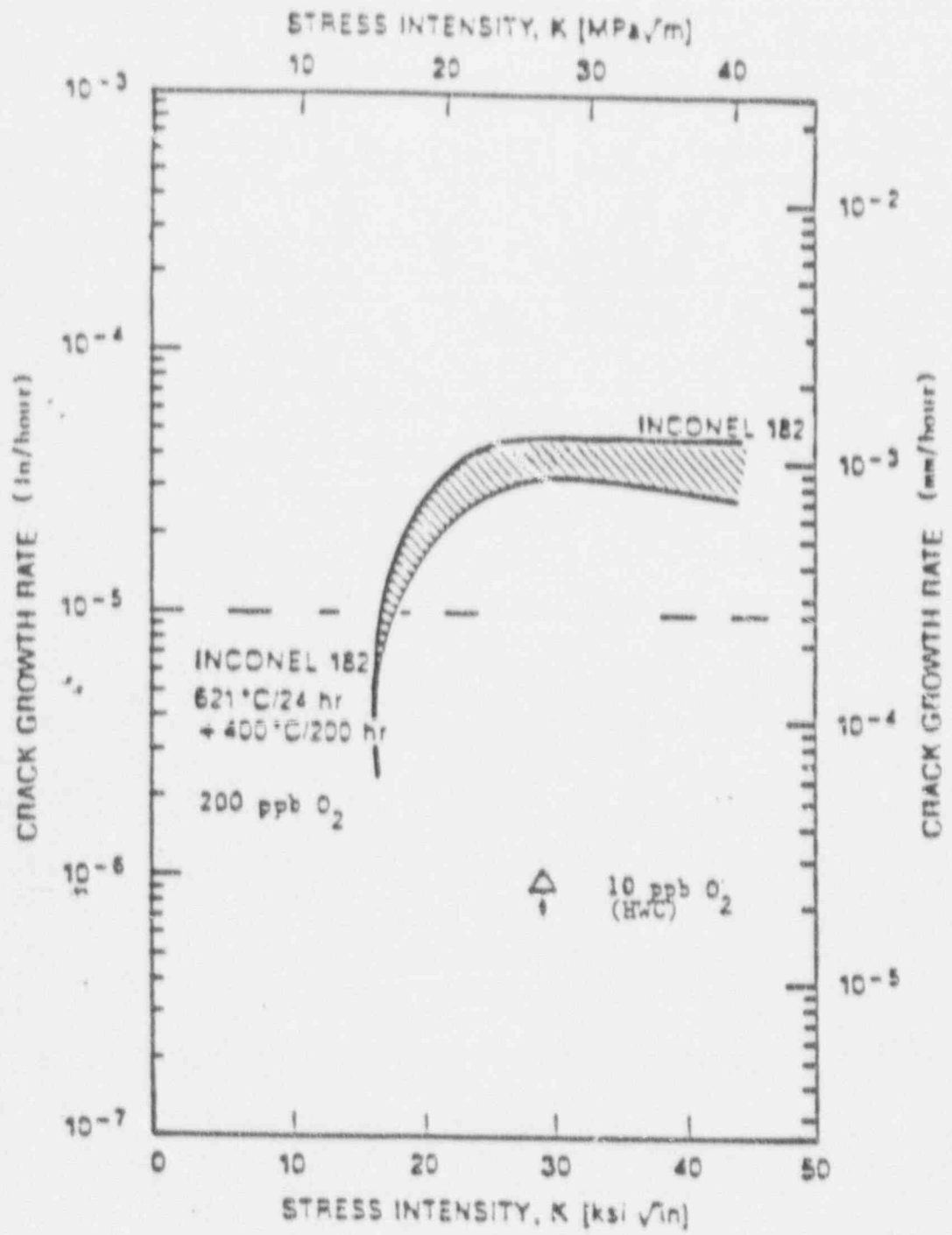| DATA TYPE	TEST NO.	SPECIMEN TYPE	LOADING TYPE	CONDUCT.	OXYGEN (ppm)	MATERIAL CONDITION	K (ksi-in$^{.5}$)	da/dt (in/hr)	COMMENTS
HALE	1	1TCT	ACTIVE	0.50		PWHT+LTS	23.2	3.3e-5	crack growth measured by compliance;
"	2	"	"	0.45			32.1	4.0e-5	heat treatment: 1150F/24 hours/air cool+
"	3	"	"	0.45			39.9	3.7e-5	750F/24 hours/air cool
HORN	1	1TWOL	DISPL.	0.5	0.2	AW	14.0	1.0e-5	conductivity estimated; incubation
"	2	"	"	"	"	PWHT	14.0	7.7e-6	period assumed as zero.
"	3	"	"	"	"	AW	14.0	5.9e-6	
JEWETT	1	CT	ACTIVE	0.47		PWHT	41.0	4.2e-5	heat treatment:1150F/24 hours plus air cool.
BENSCH	1	0.9TCT	ACTIVE	0.50		PWHT+LTS	16.0	4.0e-5	slow cyclic loading before applying constant load.
WALKER	1	1TCT	ACTIVE	0.50	0.01	PWHT+LTS	35.0	4.3e-5	3 cycles/day for compliance measurement
ANDRESEN	1	CT	ACTIVE	0.10	7.0	AW	30.0	4.1e-5	tria. wave loading. R=0.6
"	2	"	"	"	"	"		9.5e-6	constant load. R=1.0
"	3	"	"	"	"	"		1.7e-5	1 cycle/hour. tria. wave. R=0.6
"	4	"	"	"	0.2	"		1.5e-6	constant load. R=1.0
"	5	"	"	"	"	"		3.0e-6	tria. wave loading. R=0.7
"	6	"	"	1.00	"	"		4.1e-6	tria. wave loading. Sulfate added
"	7	"	"	"	0.01	"		4.0e-7	tria. wave loading. sulfate added
CAV	1	CT	ACTIVE	0.15		PWHT	24.0	1.7e-5	plant HI
"	2	"	"	0.15		"	27.0	1.5e-5	plant BI
"	3	"	"	0.30		"	27.0	3.1e-5	plant BZ. instantaneous rate
"	4	"	"	0.15		"	28.0	1.9e-5	plant DA
"	5	"	"	0.15		"	28.0	1.2e-5	plant F
"	6	"	"	0.10		"	31.0	1.2e-6	plant LI

Figure 3-1 Inconel-182 Weld Metal Crack Growth Rate.

Figure 3-2

Crack Growth Rate of Alloy 182
Function of Conductivity

Crack Growth Rate (µin/h)
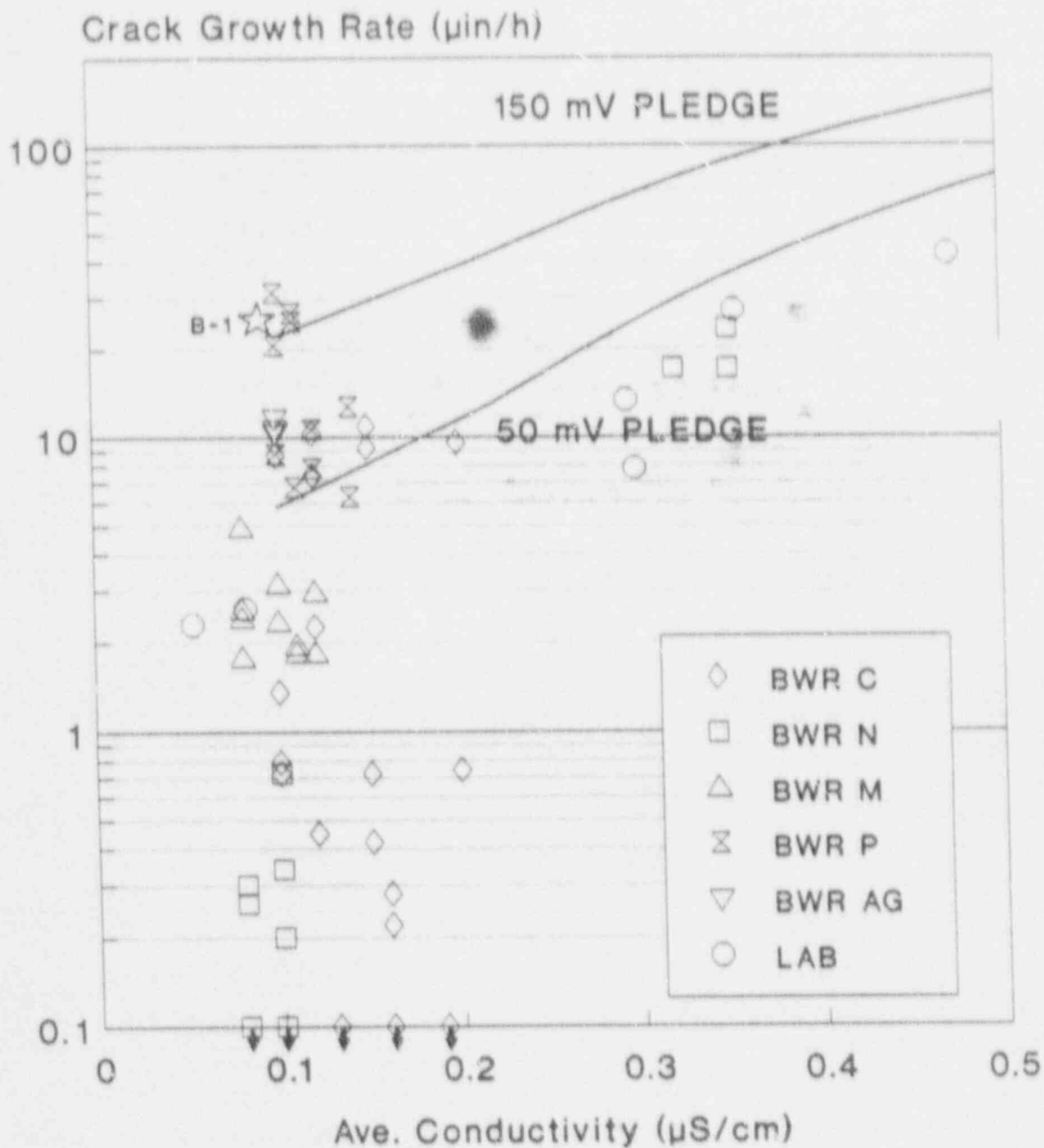
BWR K • 25-29 ksi√in
LAB K • 39 ksi√in

Solid points • HWC

4.0 WELD TOUGHNESS CONSIDERATIONS

The indication in Nozzle N4A weld is located on the safe end side of the Alloy-182 butter. The Alloy-182 weld metal is nominally a stick weld deposited using a flux. Unlike stainless steel flux welds where experimental data show significant degradation (especially for SAW material) in fracture toughness, there is no reason to expect similar reduction in toughness in the Alloy-182 welds.

To account for the reduced toughness of the stainless steel flux welds, the allowable flaw sizes in the ASME Section XI Code procedures are based on the elastic-plastic fracture mechanics (EPFM) methods. The material toughness information in the EPFM methods is specified in the form of the material J-T curve. Under EPRI sponsorship, GE has conducted testing to obtain material J-T curves and Charpy energy values for stainless steel flux welds [4-1]. The GE stainless steel flux weld J-T curves correlate very well with the J-T curve assumed in the development of the ASME Section XI Code procedures.

Although the EPFM methods use only the material J-T curve information, the Charpy energy and lateral expansion are also good indicators of the material toughness. Therefore, Charpy tests on the Alloy-182 weld specimens were conducted and the results compared with the stainless steel flux weld results. The main objective of the testing was to show that the Alloy-182 failure mode is ductile and that the toughness is better than that used in the Code for SAW stainless steel weld metal.

Three Charpy tests each at room temperature and at 550° F were conducted. All of the fractures, both at room temperature and at 550° F, in the Alloy-182 specimens were ductile. Figure 4-1 shows the photograph of the fracture surface of the Charpy specimen tested at 550° F. Table 4-1 summarizes the Charpy energy and lateral expansion results from these tests. It is seen that the Charpy energies (CVNs) at 550° F range from 69 to 80 ft-lbs and the lateral expansions range from 51.5 to 56 mils. While both the CVN and the lateral expansion represent meaningful measures of material ductility, the lateral

expansion is believed to be a more accurate indicator of toughness. For comparison, the Table 4-1 also shows the results for the stainless steel flux welds obtained in Reference 4-1. It is seen that the Alloy-182 test results are better especially on the basis of lateral expansion values when compared to the stainless steel SAW welds.

4.1   Reference

4-1 Horn, R.M., Mehta H.S., Andrews, W.R. and Ranganath, S., "Evaluation of the Toughness of Austenitic Stainless Steel Pipe weldments," EPRI Report No. NP-4668, June 1986.

TABLE 4-1

Charpy Energy and Lateral Expansion Values from Tests on Alloy-182 weld specimens

Material	Sample #	Temperature (°F)	Energy (Ft-Lbs)	Lateral Expansion (mils)
Alloy-182	1	68	62	44
"	2	68	52	48
"	3	68	71	45
"	4	550	80	52
"	5	550	69	56
"	6	550	69	55
Stainless Steel[1] Flux Welds				
SMAW	Average	550	79	84
SAW	"	550	73	33

[1]Results from Reference 4-1.

expansion is believed to be a more accurate indicator of toughness. For comparison, the Table 4-1 also shows the results for the stainless steel flux welds obtained in Reference 4-1. It is seen that the Alloy-182 test results are better especially on the basis of lateral expansion values when compared to the stainless steel SAW welds.

4.1 Reference

4-1 Horn, R.M., Mehta H.S., Andrews, W.R. and Ranganath, S., "Evaluation of the Toughness of Austenitic Stainless Steel Pipe weldments," EPRI Report No. NP-4668, June 1986.
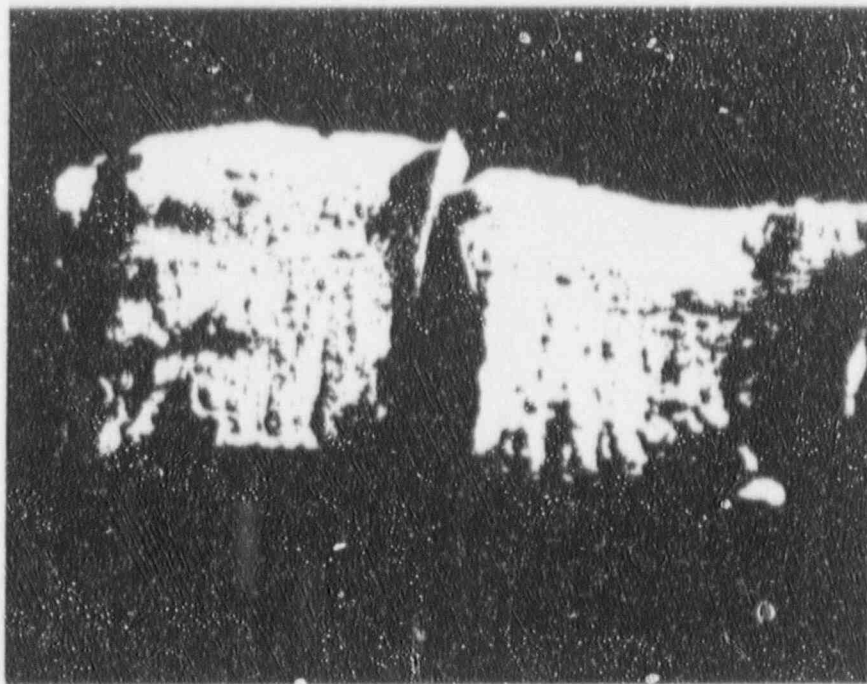
Figure 4-1 Fracture Surface of Alloy 182 Specimen No. 5

5.0 FRACTURE MECHANICS ANALYSIS

In this Section, structural margins are calculated considering the stress state at the subject weld and the projected crack growth of the indication. The methodology used is consistent with Paragraph IWB-3640 and Appendix C of Section XI of the ASME Code [5-1]. References 5-2 and 5-3 were used as major inputs in developing the Code methodology. Although initially used in mostly austenitic stainless steel applications, the Code procedures also cover, per Paragraph IWB-3641, the Ni-Cr-Fe alloys (e.g., Alloy 600) and the associated weld metals (e.g., Alloy-182 and Alloy-82).

5.1 Applied Stress Magnitudes

Figure 5-1 shows the geometry of the safe end and the nozzle. The subject indication is located on the safe end side of the Alloy-182 butter. The Alloy-182 weld metal is nominally a stick weld deposited using a flux. Unlike stainless steel flux welds where experimental data show degradation in fracture toughness, there is no reason to expect similar reduction in toughness for the Alloy-182 welds. The limited Charpy tests described in Section 4 confirm the ductile behavior of Alloy-182. Nevertheless, we will conservatively use the flux weldment rules given in Reference 5-1 to determine the allowable flaw size. In determining the allowable flaw sizes at flux weldments, the stresses from both the primary loads and the thermal expansion loads are utilized.

The stresses were calculated from the forces and moments supplied by GSU based on the stress report for the subject piping system. The piping stress report had listed the forces and moments at a mathematical node point 1.133 ft outboard from the weld N4A. Therefore, the bending moments at the weld were calculated by accounting for this difference. Table 5-1 shows the calculated values of nominal membrane and bending stresses for various loads.

5.2 Flaw Assessment Diagram

The flaw assessment diagram shows the allowable flaw sizes and the projected growth of the indication to the end of operating cycle. Methods provided in

Reference 5-1 were used to determine the allowable flaw sizes. The subject indication is located in the Alloy-182 butter on the safe end side. Since the Alloy-182 in the butter is deposited by a flux process, the formulas prescribed for the flux welds in Reference 5-1 were used.

Figures 5-2 and 5-3 show the allowable flaw size curves obtained using the P_m, P_b and P_e values derived from the piping stresses listed in Table 5-1. The allowable flaw curve in Figure 5-2 was obtained considering Level A and B conditions loads and is thus based on a safety factor of 2.77. The loads included in the analysis were pressure, weight, OBE and thermal expansion (see Table 5-1).

The allowable flaw curve in Figure 5-3 is based on a safety factor of 1.39 and the Level D condition loads which included pressure, weight, thermal expansion and a conservative combination of SSE, Annulus Pressurization and fluid transient loads. Of the two allowable flaw curves, the one that gives smaller allowable flaw sizes was used for the flaw assessment purpose. An inspection of Figures 5-2 and 5-3 shows that the two allowable flaw curves are very close but Figure 5-3 gives slightly smaller allowable flaw sizes. Therefore, Figure 5-3 was used in the flaw assessment. It is seen in Figure 5-3 that the subject butt weld can tolerate a through-wall circumferential crack 25% of the circumference long ($\approx$ 11 inches) and still maintain Code required structural margins.

5.3 Projected Crack Depth at the End of Current Cycle

The crack depth and length measured by UT at the refueling outage 3 [RF3] was 0.33 inch and 7.7 inches, respectively. The measured values during the March 1990 mid-cycle inspection were 0.2 inch and 6.625 inches. The preceding flaw geometries were used as the initial crack sizes in the projected crack depth assessment.

The overall crack growth at the subject weld would be a combination of cyclic fatigue crack growth and SCC growth under sustained load. The contribution of the fatigue crack growth is generally insignificant. To verify this, a conservative estimate of the fatigue crack growth was made for the current fuel

cycle. The K value for a limiting transient such as the Turbine Trip was estimated as 35 ksi√in. Based on the environmental fatigue crack growth rate data shown in Figure 16 of Reference 3-3, the fatigue growth rate was determined as 4×10^{-5} in/cycle. If 100 such transient events are conservatively assumed, the fatigue crack growth is calculated as 0.004 inch. This growth is insignificant compared to the estimated SCC growth of 0.348 inch (see next paragraph) for the current fuel cycle.

Based on the discussion presented in Section 3, a bounding SCC growth rate of 2.9×10^{-5} in/hour is used to determine the projected crack depth at the next refueling outage in March 1992. The hot operating time for the current fuel cycle was assumed as 12000 hours. The actual hot operating time is expected to be closer to 11000 hours. Using the preceding crack growth rate and the assumed 12000 operating hours, the crack is projected to grow by an increment of 0.348 inch to a depth of 0.678 inch or approximately 60% of wall (based on a nominal section thickness of 1.125 inches) at the end of the current cycle (see Figures 5-2 and 5-3). If one uses the nominal crack growth rate of 1×10^{-5} in./hour (based on the change in crack depth averaged over the period of the entire cycle), the predicted crack depth at the end of the current cycle is 0.45 inch (see Figure 5-4).

5.4 Fracture Mechanics Evaluation

As shown in Figure 5-3, the Code required structural margins can be maintained even with a through-wall crack. Nevertheless, since the continued plant operation with a potentially leaking through-wall flaw is not acceptable, the IWB-3640 procedures include an arbitrary limit on the end-of-period projected flaw depth. This arbitrary limit was specified as 75% for the austenitic base metal and non-flux welds, and 60% for the flux welds [5-4]. Figures 5-3 and 5-4 also show two dotted lines parallel to the abscissa at a/t =0.60 and 0.75.

Figures 5-3 and 5-4 show in nondimensional form the projected crack depth and length at the end of current cycle. In Figure 5-3 the projected crack depth at the end of current cycle meets the Code criteria even with the bounding crack

growth rate of 2.9×10^{-5} in/hour. The projected crack depth is only 45% (Figure 5-4) of wall if the average crack growth rate is used. Thus, it is concluded that the projected crack depth at the end of current cycle is such that the Code required structural margins are maintained even with the limiting crack growth rate assumptions. Furthermore, even if a higher growth rate is postulated, a through-wall flaw of this length can be tolerated while still maintaining the Code required safety margins. Clearly, a mid-cycle inspection to verify integrity is not necessary and continued operation to the end of the current cycle is justified.

5.5 References

5-1 ASME Boiler and Pressure Vessel Code, Section XI, 1986.

5-2 Ranganath, S. and Mehta H. S., "Engineering Methods for the Assessment of Ductile Fracture Margin in Nuclear Power Plant Piping," ASTM STP 803, Vol. II, 1983.

5-3 Ranganath, S., Mehta H.S., and Norris, D.M., "Structural Evaluation of Flaws in Power Plant Piping," PVP Vol 94, ASME 1984.

5-4 "Evaluation of Flaws in Austenitic Steel piping: Section XI Task Group for Piping Flaw Evaluation, ASME Code," Journal of Pressure Vessel Technology, Vol. 108, August 1986.

TABLE 5-1

Applied Stresses at Nozzle to Safe End Weld N4A

Loading Type	Applied Stress (Ksi)	
	Membrane Stress	Bending Stress
Pressure	3.3	0.0
Weight	0.0	0.3
Seismic (OBE)	0.1	3.6
Seismic (SSE)	0.4	11.6
Thermal	0.1	13.9

Section Properties: Outside Diameter = 14.25 in.
Inside Diameter = 12.00 in.

EXISTING
LOW ALLOY
STEEL ALLOY

INCONEL
WELD BUILDUP
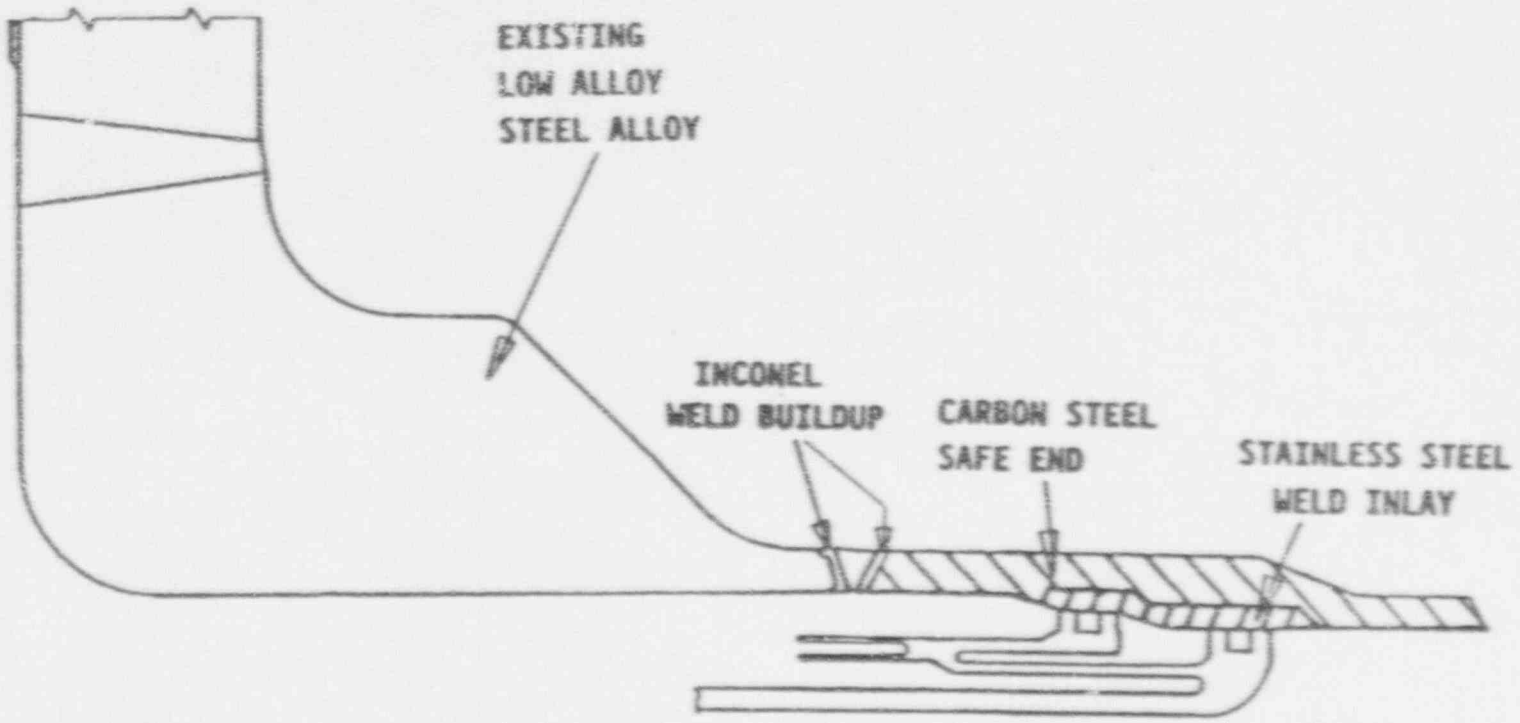
CARBON STEEL
SAFE END
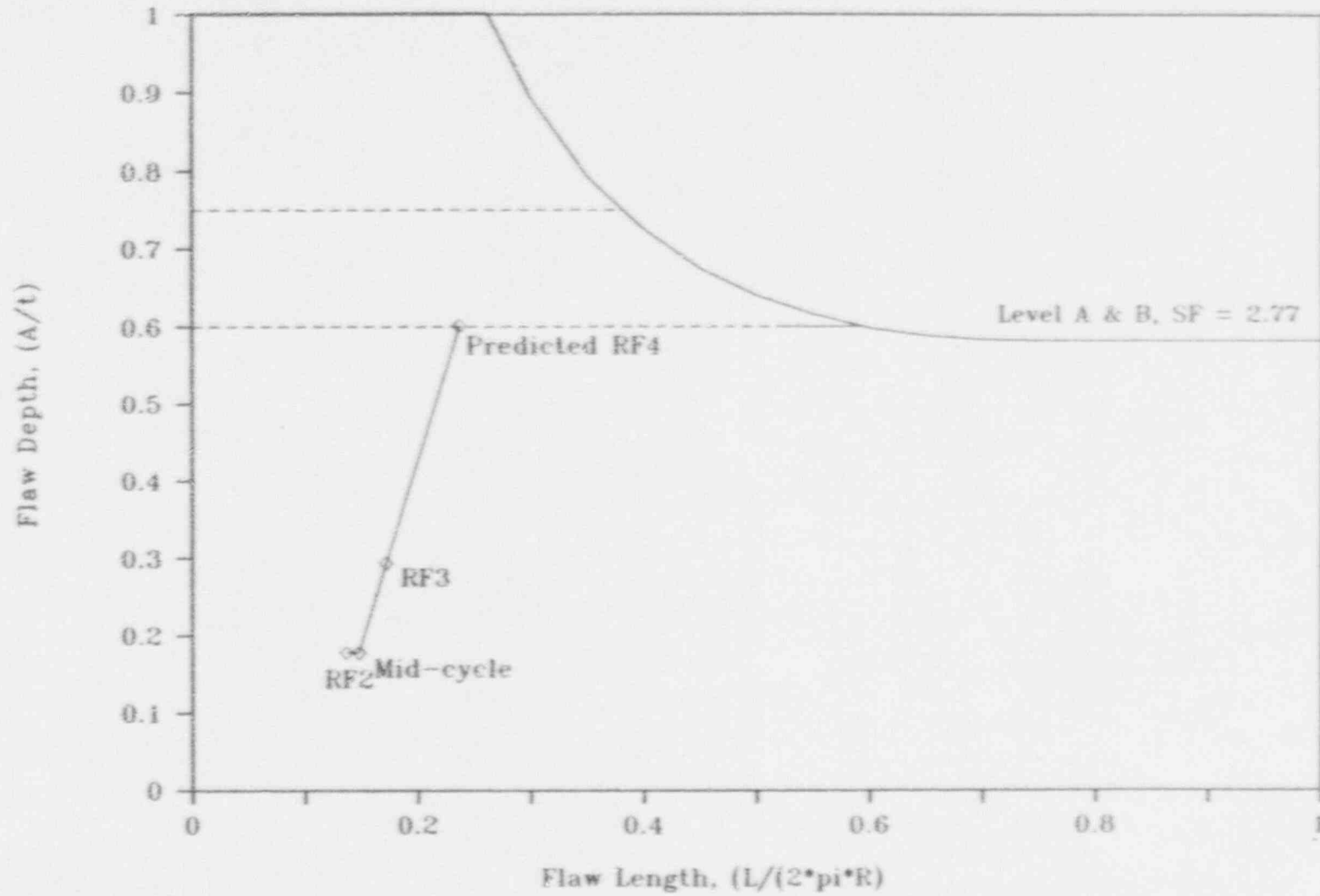
STAINLESS STEEL
WELD INLAY

Figure 5-1 Feedwater Nozzle to Safe End Weld Configuration at N4A

Level A & B Condition Flaw Assessment Diagram, River Bend — Feedwater Nozzle
Crack Growth Rate of 2.9×10^{-5} inches/hr

Figure 5-2   Flaw Assessment Diagram for Level A & B Conditions Based
on 2.9×10^{-5} in/hour Crack Growth Rate

Level D Condition Flaw Assessment Diagram, River Bend – Feedwater Nozzle
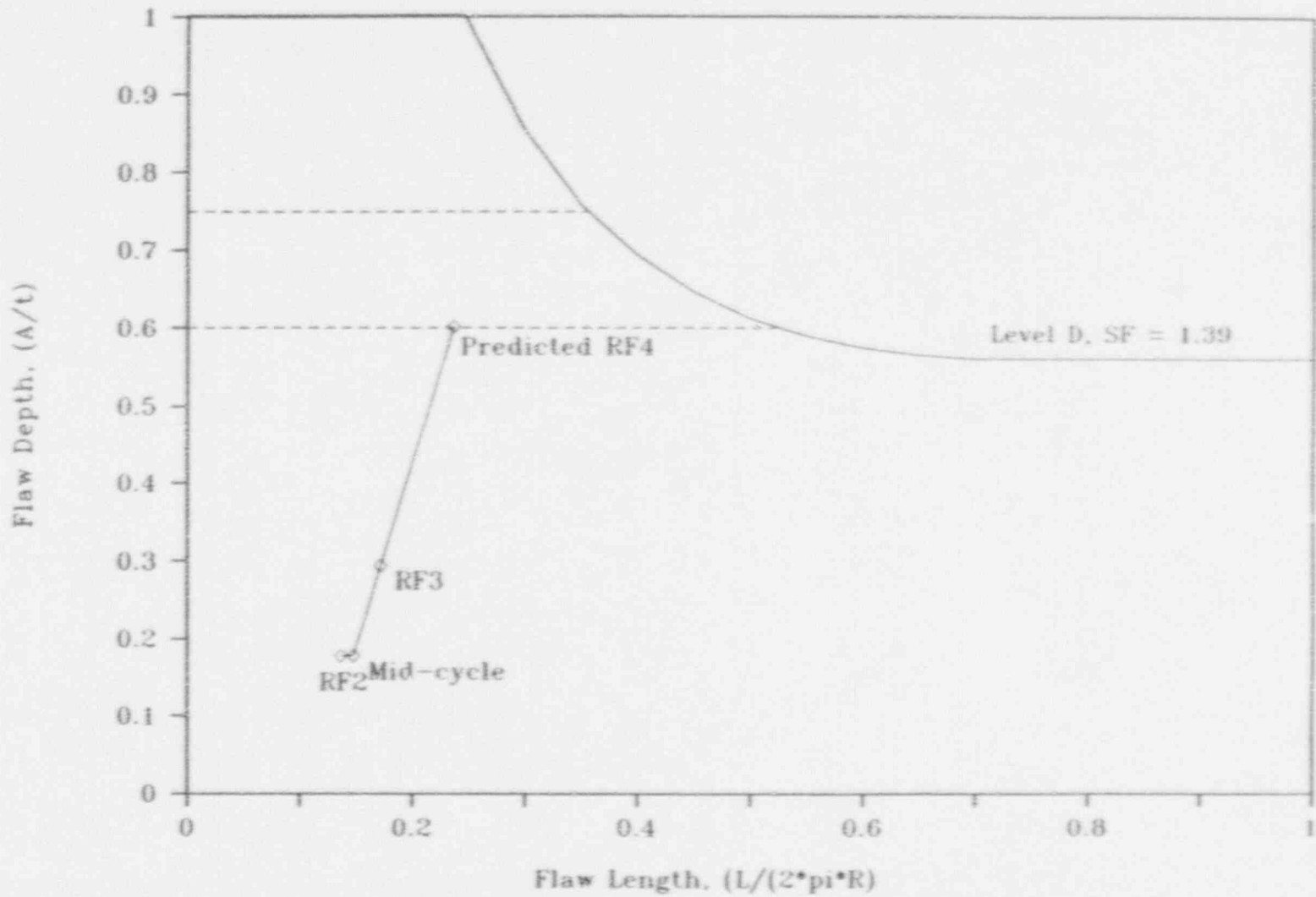## Crack Growth Rate of 2.9×10^{-5} inches/hr

Figure 5-3 Flaw Assessment Diagram for Level D Conditions Based
on 2.9×10^{-5} in/hour Crack Growth Rate

Level D Condition Flaw Assessment Diagram, River Bend – Feedwater Nozzle

Crack Growth Rate of 1.1×10^{-5} inches/hr
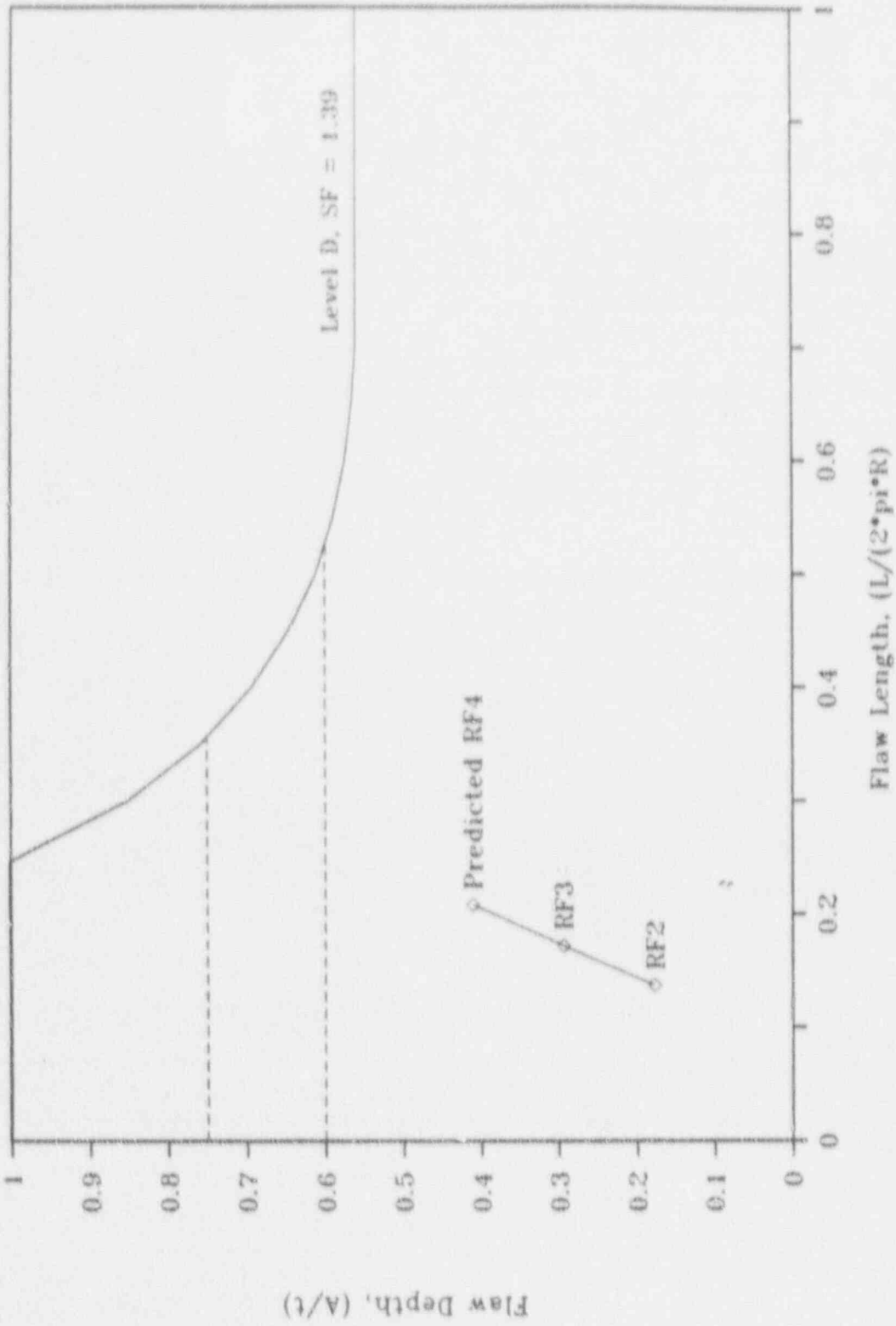
Level D, SF = 1.39

Predicted RF4

RF3

RF2

Flaw Length, $(L/(2 \cdot pi \cdot R))$

Flaw Depth, (A/t)

Figure 5-4 Flaw Assessment Diagram for Level D Conditions Based on 1.0×10^{-5} in/hour Crack Growth Rate

6.0 LEAK-BEFORE-BREAK ASSESSMENT

The objective of the leak-before-break (LBB) assessment is to determine the structural margins at the subject weld in the unlikely event that the indication should propagate through-wall during the current fuel cycle. The LBB methodology is generally applied to high energy fluid piping systems to demonstrate that they are unlikely to experience double-ended ruptures. Some of the fracture mechanics techniques for use in the LBB assessments and the criteria are outlined in NUREG-1061 [6-1] and in General Design Criteria 4 [6-2]. The LBB approach has been successfully used in Light Water Reactor (LWR) applications to eliminate postulated double-ended break requirement and thereby provide a sound technical basis to eliminate hardware associated with postulated pipe whip and jet impingement effects.

The purpose in conducting the LBB assessment for this evaluation was not the elimination of the double-ended break requirement but to estimate the inherent margin between the through-wall flaw length that can be detected by the leakage monitoring systems in place at River Bend Station and the flaw length or the critical crack length that could lead to unstable crack extension.

The two key calculations in a LBB assessment are: (1) calculation of leak rate as a function of through-wall crack length, and (2) determination of critical through-wall crack length based on material fracture toughness and applied loadings. Details of these calculations and the LBB margins are discussed next. It is shown that large LBB margins exist at this weld.

6.1 Leak Rate Calculation

Leak rates of high pressure fluids through cracks in pipes are a complex function of crack geometry, crack surface roughness, applied stresses, and inlet fluid thermodynamic state. Analytical predictions of leak rates essentially consist of two separate tasks: (1) the estimation of

the fluid flow rate per unit area and, (2) calculation of the crack opening area. The first task involves the fluid mechanics considerations in addition to the crack geometry and its surface roughness information. The second task requires the fracture mechanics evaluation based on the piping system stress state.

The methodology used in the leak rate calculation is described in Reference 6-3. A comparison of the leak rates predicted by this methodology and those predicted by the PICEP computer program [6-4] showed good agreement. Also, a good correlation was obtained between the field observed leak rate from a creviced safe end at the Duane Arnold plant and the prediction using this methodology as shown in Figure 6-1. The observed leak rate is bounded by the two curves (one used no contribution from bending moment and the other used maximum contribution from bending moment).

Only the steady state piping loads are considered in the leak rate calculation. Thus, the piping loads included in the leak rate calculation were internal pressure, weight and thermal expansion. Figure 6-2 shows the calculated leak rates as a function of through-wall circumferential crack length.

In the next Subsection, the predicted leak rates in Figure 6-2 are compared with the detection capability at River Bend Station.

6.2 Leak Detection Capability

The total leakage inside the containment consists of identified leakage and unidentified leakage. The identified leakage is that from the pumps, valve stem packings, reactor vessel head seal and upper containment pool liner, and bellow seal, which all discharge to the equipment drain sump. The unidentified leak rate is the portion of the total leakage received in the drywell sumps that is not identified with any of the sources listed in the preceding. With the implementation of new technical specifications, the leakage detection

capability at River Bend Station will meet the requirements of Regulatory Guide 1.45 [6-5] and Generic Letter 88-01 [6-6]. Initiation of shutdown action and drywell entry would be required when the unidentified leak rate exceeds 5 gpm or shows an increase of 2 gpm in any 24 hour period.

Typical unidentified drywell leakage at River Bend during fuel cycle 4 has been in the range of 0.1 to 0.2 gallons per minute. In view of the small unidentified leakage rate at River Bend, any change in this rate due to a potential through-wall crack would be readily detected. The new leakage limits will also assure prompt detection should the subject indication grow through-wall between now and RF-4.

6.3 Instability Crack Length

The instability crack length can be calculated using the J-integral and the associated tearing modulus crack stability criterion. In fact, such calculations were the basis of the acceptance criteria for austenitic flux welds [6-7]. The simplified closed form expressions for the allowable flaw sizes were developed in Reference 6-7 to bound the predictions using the J-integral method. These closed form expressions are summarized in Appendix C of Section XI. Therefore, these expressions with safety factor defined as 1.0, were used to calculate the instability crack length for this case.

Using the preceding approach, the critical crack length was calculated as 15.2 inches. The LBB structural margins are evaluated next.

6.4 LBB Structural Margin Assessment

From Figure 6-2, the leakage crack length corresponding to 5 gpm leak rate is approximately 4.6 inches. The critical crack length was calculated as 15.2 inches in the preceding subsection. Thus, the ratio of the 5 gpm crack length to critical crack length is (15.2/4.6) or 3.3. This value is considerably more than the minimum value of 2.0 required in typical LBB analyses.

The preceding margin clearly demonstrates that in the unlikely event that the subject indication develops into a through-wall crack, the resulting leakage

will be detected well before the crack length could approach critical value that could lead to failure of the weld.

6.5 References

6-1 Report of the U.S. Nuclear Regulatory Commission Piping Review Committee: Evaluation of Potential for Pipe Breaks, NUREG-1061, Volume 3, US NRC, Washington D.C., November 1984.

6-2 Amendment to General Design Criterion 4, Broadscope rules, Federal Register/Volume 52, No. 207, October 27, 1987.

6-3 Mehta, H.S., "Determination of Crack Leakage Rates in BWRs," GE Report, April 1985.

6-4 D.M. Norris, A. Okamoto, B. Chexal and T. Griesbach, "PICEP: Pipe Crack Evaluation Program," EPRI Report No. NP-3506-SR, August 1984.

6-5 Regulatory Guide 1.45, Reactor Coolant Pressure Boundary Leakage Detection Systems, May 1973.

6-6 NRC Generic Letter 88-01: NRC Position on IGSCC in BWR Austenitic Stainless Steel Piping January 1988.

6-7 "Evaluation of Flaws in Austenitic Steel piping: Section XI Task Group for Piping Flaw Evaluation, ASME Code," Journal of Pressure Vessel Technology, Vol. 108, August 1986.
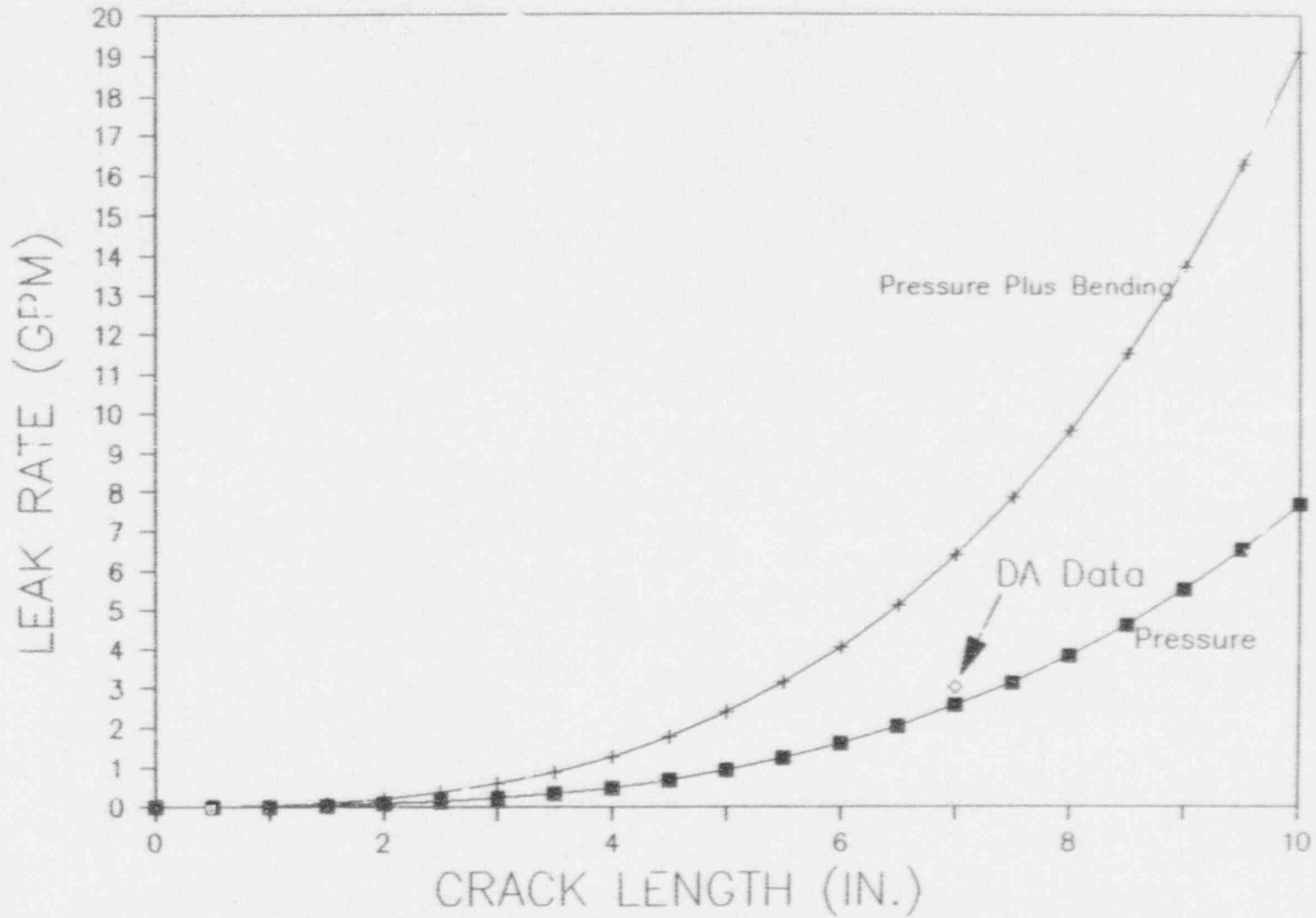
Figure 6-1 Comparison of Observed Leak Rate with the Predicted Leak
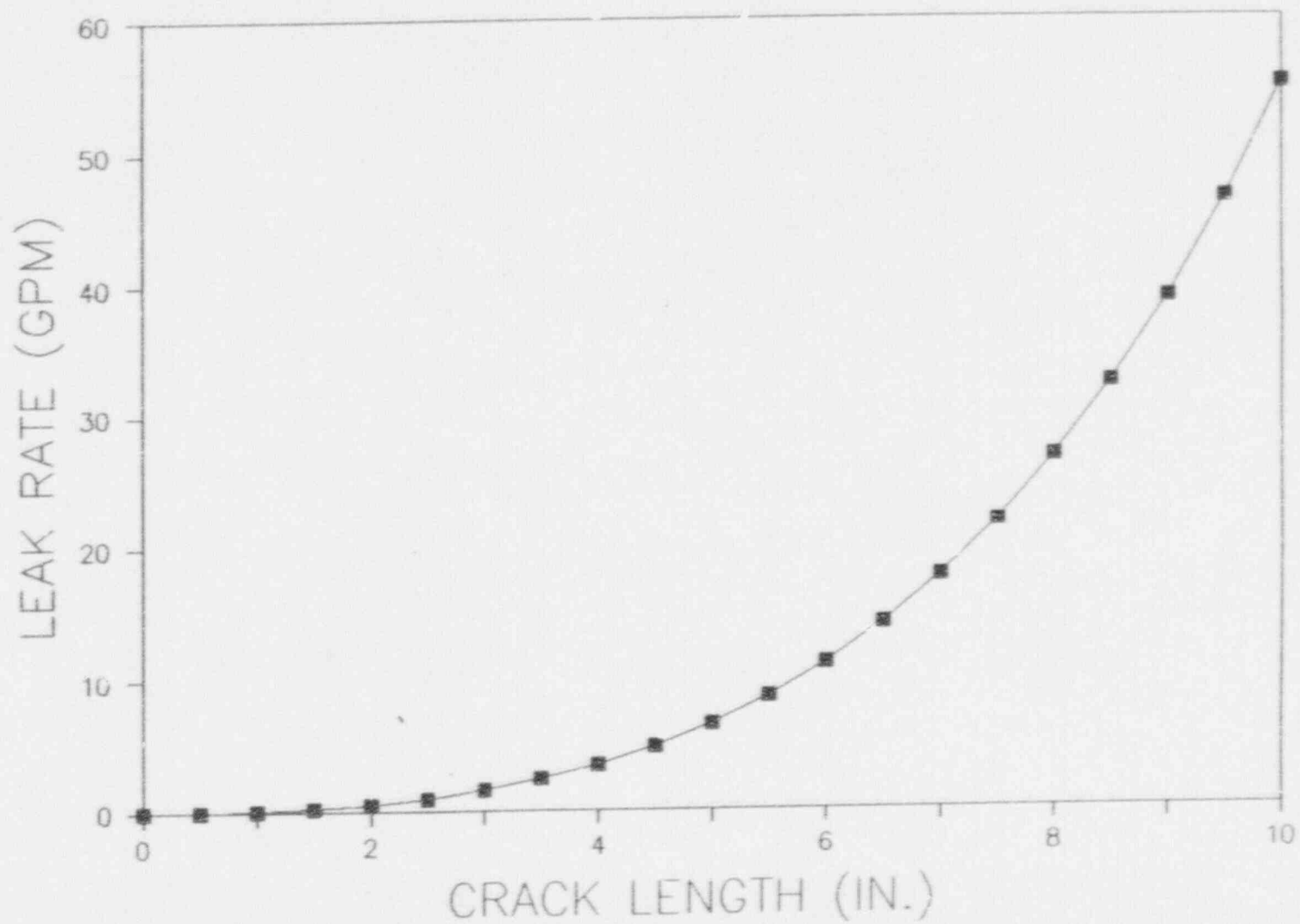Rate Using GE Computer Program

Figure 6-2 Predicted Leak Rate as a Function of Crack Length at N4A Weld

7.0 SUMMARY AND CONCLUSIONS

This report provides the technical justification for the elimination of the planned mid-cycle inspection of the indication in the River Bend feedwater nozzle to safe end weld. The evaluation performed in November 1990 confirmed that continued operation for the current cycle could be justified. Nevertheless, to provide additional conservatism, GSU had planned on performing the mid-cycle inspection in September 1991. The technical justification described here and the planned GSU actions for the March 1992 outage, have made the mid-cycle inspection unnecessary. The specific conclusions from the structural evaluations are summarized here.

o Flow visualization tests confirm that crevice conditions do not exist in the feedwater thermal sleeve annulus.

o Crack growth rates in the Alloy-182 weld were estimated using three approaches:

   (i)   Based on the UT measurements
   (ii) Based on predictions of the GE IGSCC model
   (iii) Based on available in-reactor CAVS data

   All three methods provide consistent estimates with a limiting value of 2.9×10^{-5} in/hour.

o Fracture mechanics evaluations confirm that even with the conservative ASME Code flux weld criteria, and limiting crack growth rate assumptions, continued operation through the current cycle can be justified and the Code margins maintained.

o A leak-before-break assessment was performed to determine the structural margins associated with a through-wall crack. It was found that even if the crack growth rate were higher and the crack became through-wall, the Code structural margins would still be maintained.

Furthermore, the expected leak rate for a potential through-wall crack is well in excess of the limit for unidentified leakage rate, so that the crack would be readily detected.

GSU has taken and will take several actions which will significantly reduce the need for, as well as the value of, a mid-cycle inspection. These actions include:

o   Plans to impose more restrictive technical specification limits on unidentified leak rate. This will provide added assurance of leak margin so that even under the most unlikely circumstance of the crack growth being excessive, a potential leak could be detected readily.

o   Added emphasis on maintaining the water chemistry to assure that the BWR Industry/EPRI guidelines are not only met but improved upon.

In view of these corrective actions and the radiation exposure, as well as, the added plant downtime resulting from the inspection, the mid-cycle inspection is unnecessary. This is especially true when one considers the fact that the indication has been shown to be acceptable for continued operation through March 1992.